Novel Heartbeat Detection Method in Presence of Large-Scale Random Body Movement Using SFCW Radar: A Simulated Study

Yu Rong and Daneil Bliss
School of Electrical, Computer and Energy Engineering
Arizona State University
Tempe, AZ
yrong5@asu.edu

***Abstract*—This paper introduces a novel signal processing method for wideband radar system to estimate heart rate in presence of large random body movement. The new method estimates the bulk body motion prior to range transformation by dividing the wideband signal into multiple narrowband continuous waves. Each subband is used to obtain a coarse estimate then combined to produce a refined estimate. The heart rate is indirectly estimated from radar heart sound signal by looking at the heart sound repetition frequency. Since the heart sound signal is mainly located at much higher frequencies than the fundamental heartbeat frequency, the final body motion estimate is low-passed version of the refined estimate to preserve the high frequency heart sound. The motion cancellation occurs at complex signal domain after locating the targeted range bins of interest without the need of judicious phase calibration. The proposed theory is validated using a simulated K-band stepped-frequency continuous wave radar system. Monte carlo simulation study shows that the developed signal processing technique and heart sound recovery based heart rate estimation almost achieve perfect accuracy in presence of large-scale body motion.**

***Index Terms*—Remote sensing, random body movement, signal processing, SFCW, vital signs**

I. Introduction

Radar technologies for vital sign measurement have the potential to greatly improve patient experiences and practitioner safety while creating the opportunity for comfortable continuous monitoring [1]. The feasibility of heath radar has been established a few decades ago [2]. Since then significant research has been efforts devoted to developing and promoting radar signal processing and systems for contactless vital signs [3]. Up to now, requirement for robust sensing in more realistic scenarios, such as free-living, still prevent radar technology from widespread use in our daily life [4].

This paper investigates an important issue in radar based vital signs detection in presence of large-scale random body movement (RBM). The focus of this paper is developing signal processing approach for RBM without complicated system and auxillary sensors. Existing active RBM cancellation methods either require complex system setup [5]–[7]. For example, [5] demonstrated dual continuous wave radars placed at front and back sides to cancel out RBM. [8] performed similar experimental setup but exploiting self-injection-locked Doppler radar technique. [6] exploited external camera sensor to estimate body motion and fuse with radar in order to cancel RBM. Another attempt [7] showed dual-ultra-wideband inpulse radar strategically placed at tilted angles to achieve RBM cancellation.

The proposed signal processing method is developed using stepped-frequency continuous wave (SFCW) signal model. And it can be readily generated to other wideband radar using frequency-modulated continuous wave (FMCW). RBM even for quasi-stationary subject generates spectral spread, masking the vital signs frequency features at very low frequency range close to DC. The conventional phase based methods cannot handle motion interference in vital signs detection since body motion introduces dynamic DC-offset [9]. Existing DC-offset calibration methods [10] assume static offset and thus fail to function. The phase errors after offset calibration can leak into the frequency range of vital signs and the leakage spread depends the RBM velocity. For large-scale RBM, the residual phase errors are proportional larger. The corresponding displacement error can overwhelm the vital signs motion.

Contributions:

- Develop a novel RBM cancellation technique for wideband SFCW radar
- Incorporate parametric heart sound model development in [11]
- Estimate heart rate indirectly from high frequency heart sound
- Develop a simulation tool to evaluate the impact of RBM on heart sound recovery

II. Radar Heart Sound Based Heart Rate Estimation

A. Radar Heart Sound Model

A radar heart sound signal model is briefly described and adopted from [11]. Having an precise heart sound model aids in signal analysis method development.

This model captures the general structure of each individual radar heart sound and derived from actual radar heart sounds from several subjects. Each cardiac cycle consists of two

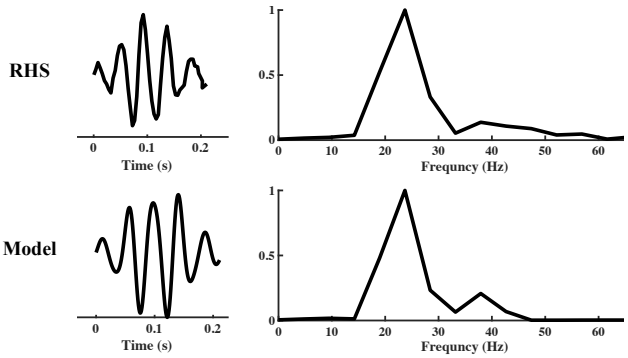

Fig. 1. Individual radar heart sound (RHS) compared in time and frequency with model heart sound. The stronger lower frequency component and weaker higher frequency component can be seen in both signals.

distinguishable heart sounds, S_1 and S_2. In the time domain the time duration, peak amplitude and separation between each heart sound vary subject to subject. Visual inspection of individual heart sounds indicate that they reach peak value in the center of the heart sound and taper in a Gaussian shape. In the frequency domain. Each individual heart sound is found to consist of two main frequency components. One very strong lower frequency component in the 20-30 Hz range and one much weaker component in the 30-50 Hz range.

To capture both main frequency components and their respective strengths, the underlying signal is modelled as a sum of two weighted sine waves. A Gaussian window is applied to taper the shape of the model waveform to resemble the shape of the of the radar heart sound. The modeled heart sound is given as,

$$x(t) = w(t)\sin(2\pi f_1 t) + .2\,w(t)\sin(2\pi f_2 t), \tag{1}$$

where f_1 and f_2 are the strong and week frequency components respectively and $w(t)$ is the windowing function given as,

$$w(t) = P\,e^{-\frac{t^2}{2\sigma^2}} \tag{2}$$

Where P is the peak amplitude of the respective heart sound, and $\sigma = T_s/2$ with T_s being the time duration of the heart sound. The spacing, time duration, frequency components and amplitudes of the model are parameterized.

B. Heart Rate Estimation

Due to the close vicinity of the vital signs, including heartbeat and respiration, to the DC. Additionally, the RBM generates wide spectral spread and masks the vital signs. The heart rate is indirectly estimated from the repetition frequency of the heart sound signal. The spectrogram of heart sound signal reveals the distinct heart sound events S_1 and S_2 in a repeated fashion. From our previous study [12], the major radar heart sound energy is roughly located about 20 Hz. In the heart sound spectrogram, a 1-D slice along time axis at 30 Hz is selected to produce an estimate of the pulse signal. The first dominant spectral peak location gives the heart rate estimate.

III. SFCW Signal Processing

A. Vital Motion Extraction

Radar system deploys a SFCW signaling and operates in the frequency domain. The SFCW radar transmits a series of discrete narrow band pulses in a stepwise manner to achieve a larger effective bandwidth. The modulated waveform consists of a group of N coherent pulses with pulse duration T, and frequencies $f_{\rm n} = f_0 + n\Delta f$. Assume that each SFCW waveform has N pulses called one SFCW frame and the center frequency of the first pulse is f_0, as illustrated in Fig. 2.

One transmitted SFMCW frame is represented as a sum of N windowed narrow band signals,

$$x_{\rm tx}(\tau) = \frac{1}{\sqrt{T}} \sum_n \text{rect}\left(\frac{\tau - nT}{T}\right) \mathrm{e}^{j2\pi(f_0 + n\Delta f)\tau}. \tag{3}$$

The backscattered SFCW frame in baseband is modeled by concatenating the down converted received pulses. The received pulse is an attenuated and delayed version of the transmitted pulse at a nominal distance R_0. However, a slowly time-varying delay is expected due to target motion, $R_T(t)$ is a function of slow-time t,

$$\tau_{\rm D}(t) = 2\,\frac{R_0 + R_T(t)}{c}, \tag{4}$$

where c denotes the speed of light. For example, the m-th frame of received waveform is written as,

$$x_{\rm rx}(t = m\,N\,T, \tau = n\,T) = x_{\rm rx}(m,n) \tag{5}$$

$$= e^{j2\pi f_0 \tau_{\rm D}(m)}\; e^{-j2\pi n\Delta f \tau_{\rm D}(m)}. \tag{6}$$

The range profile is obtained by performing inverse Fourier transform of the N fast frequnecy samples with respect to n for every frame. Then, the normalized baseband slow-time (m) versus fast-time (k) data matrix is computed as,

$$X_{\rm rx}(m,k) = e^{-j\pi(k-k_m)(N-1)/N}\; \frac{\sin[\pi(k-k_m)]}{\sin[\pi(k-k_m)/N]}\; e^{j2\pi f_0 \tau_{\rm D}(m)}. \tag{7}$$

The phase information directly related to motion of interest is preserved in the term $e^{j2\pi f_0 \tau_{\rm D}(m)}$. To extract signal of interest with maximum SNR, one fast-time delay sample (range sample) is selected across slow-time frames as $k = k_m$, which is computed as the ceiling of $\tau_{\rm D}(m)N\Delta f$, since $|X_{\rm rx}(m,k)|$ achieves its maximum as $k = k_m$.

The normalized baseband signal at the target range gives,

$$X_{\rm rx}(t) = e^{j\frac{4\pi f_0 R_T(t)}{c}}. \tag{8}$$

B. Random Body Movements

With RBM, the human body generates much stronger response in the radar receiver as the radar cross section and motion displacement magnitude increased significantly compared to the stationary case. The radar captures RBM $b(t)$, vital motion $v(t)$, including respiration and heartbeat, and heart sound induced surface skin motion $h(t)$. The target motion is

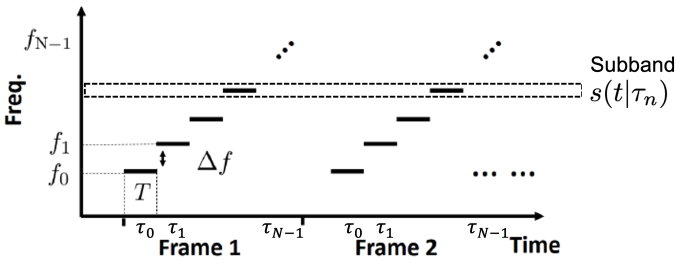

Fig. 2. Stepped FMCW radar transmission scheme.

sum of the three types of motions, $R_T(t) = b(t)+v(t)+h(t)$. The baseband signal model of the composite signal gives,

$$\begin{aligned} X_{\rm rx}(t) = e^{j\frac{4\pi f_0(b(t)+v(t)+h(t))}{c}} \\ e^{j\frac{4\pi}{c}b(t)}e^{j\frac{4\pi}{c}v(t)}e^{j\frac{4\pi}{c}h(t)} \\ e^{j\frac{4\pi}{c}l(t)}e^{j\frac{4\pi}{c}h(t)}, \end{aligned} \tag{9}$$

where $l(t) = b(t) + v(t)$ denotes the low-frequency body motion. Existing radar methods estimate heart rate relies on spectral analysis. The spectral peaks at the heartbeat frequency region of interest are the estimation candidates. But this is not feasible and RBM will mask $v(t)$. The spectral support of RBM can extend beyond a few Hz depending on the radar carrier frequency and body motion speed. The major radar measurable heart sound frequency resides above 20 Hz. Due to the convolution effect, the heart sound frequency will be shifted as much as the Doppler frequency induced by RBM velocity in Eqn. 10. To successfully recover heart sound frequency and then estimate heart rate from it, a deconvolution method is required. This is accomplished by the motion cancellation technique.

$$\begin{aligned} S(f) &= \mathcal{F}\{e^{j\frac{4\pi}{c}l(t)}e^{j\frac{4\pi}{c}h(t)}\} \\ &= \mathcal{F}\{e^{j\frac{4\pi}{c}l(t)}\} * \mathcal{F}\{e^{j\frac{4\pi}{c}h(t)}\} \end{aligned} \tag{10}$$

IV. RBM Cancellation Technique

The RBM cancellation directly operates on SFCW frequency data samples prior to range $iFFT$. The ideal of multifrequency based phase tracking developed in [13] for FMCW is invoked and modified for this problem. The SFCW signal frame is decomposed into multiple narrowband CW signals as seen in Fig. 2. At a fixed frequency f_i, the slow-time sampled beat signal gives,

$$\begin{aligned} s(t|\tau_n) &= e^{j\frac{4\pi p(t)}{c}(f_0+n\Delta f)} \\ &= e^{j\frac{4\pi p(t)}{c}f_n}. \end{aligned} \tag{11}$$

where $p(t)$ denotes the RBM observed in each subband. For a fixed f_n and τ_n, Eqn. 11 has the form of a phase-modulated CW radar with a frequency of f_n. For N samples per frequency sweep, parallelly N CW signals are leveraged to estimate motion displacement, from f_1 to f_N. The modulated phase signals $\phi(t|\tau_n) \approx 4\pi p(\tau)/\lambda_n$ are extracted by taking phase angles or other phase based method [14]. Overall displacement from body motion is obtained by summing and averaging n phase signals,

$$\hat{p}(t) = \sum_n \frac{\phi(t|\tau_n)}{\frac{4\pi}{\lambda_n}}. \tag{12}$$

The estimated displacement $\hat{p}(t)$ dominates the spectral and potentially spreads beyond 20 Hz. In order to recover the high frequency heart sound in the subsequent cancellation step, a moving average filter is applied to $\hat{p}(\tau)$. The number of samples M to average in the filtering is determined by the designed cut-off frequency, 20 Hz, and the SFCW frame rate, which is 1000 in the radar configuration. Thus, the final RBM estimate becomes,

$$\hat{l}(t) \approx \mathbf{f}\{\hat{p}(t), M\}, \tag{13}$$

where $\mathbf{f}$ denotes a filtering operator which returns a local M-point mean values and each mean is calculated over a sliding window of length M across neighboring elements in $\hat{p}(.)$.

Note that the RBM cancellation occurs in complex baseband, the desired signal after cancellation has the following form using Eqn. (14),

$$\begin{aligned} h_c(t) &\approx \frac{X_{\rm rx}(t)}{e^{j\frac{4\pi}{c}\hat{l}(t)}} \\ &\approx e^{j\frac{4\pi}{c}h(t)}. \end{aligned} \tag{14}$$

Thus, the FT of $h_c(t)$ reveals the meaningful heart sound signal without the convolution effect.

V. Simulation Study

A. RBM Modeling

RBM is generated with random work model in back and forth movement at a varying random pace. For evaluation purpose, the model is parameterized by two parameters maximum motion velocity in both directions, V_{max} varying from 5 to 60 mm/s and maximum motion magnitude, $M_{max} = 100\ mm$. Since the goal is to recovery heart sound signal, the other vital signs heartbeat and respiration are ignored. The heart sound signal magnitude fixed at 0.05 mm while the other vitals are heartbeat $0.5\ mm$ and respiration $2\ mm$. Each heartbeat corresponds to one heart sound cycle. The total signal length lasts for 10 s and the RBM persists the entire duration. One trial of the model is displayed in Fig. 3. Assuming the subject is located at 1 meter away. There is no signal propagation loss in the air for simplicity. The SFCW radar operates from 24 GHz with a bandwidth of 2 GHz. The SFCW signaling frame rate is 1000 Hz. The added system phase noise is controlled such that the integrated heart sound signal to the noise ratio (SNR) is 16 dB. One example spectra of the different motion signals are given in Fig. 3 (a)-(d) assuming that they are independently present at the receiver while the composite signal signal spectral is also provided in (e).

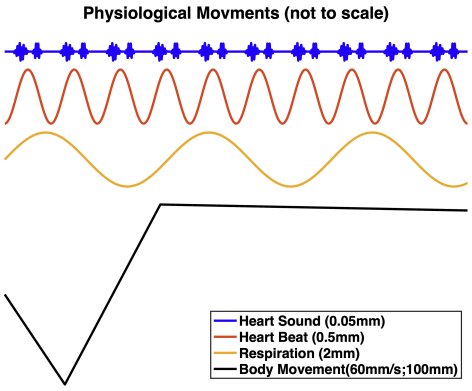

Fig. 3. Modeled physiological motion and RBM. From top to bottom, heart sound, heartbeat, respiration and RBM of a period of 10 s.

B. Heart Sound Recovery

To correctly recover the heart sound signal, the RBM signal should be firstly estimated and cancelled. Example estimated RBM spectrum corresponds to the Fig. 4(a) is given in Fig. 5(a). Following the proposed motion cancellation technique, the meaningful heart sound signatures are revealed in Fig. 5(b).

Heart sound exhibits regular time-frequency structure repeating at the heartbeat frequency. The comparison of spectrogram among the ideal heart sound signal Fig. 6(a), RMB-cancelled signal (b) and high-pass filtered one (c) confirms the effectiveness of the proposed method for heart sound recovery in presence of RBM. Naive high-pass filter simply fail because it cannot decouple the convolution effect as mentioned in Section III-B.

C. Heart Rate Estimation Performance

Computer aided simulation allows evaluation of heart rate estimation performance by varying RBM model parameters. The following Monte Carlo simulation shows the heart rate estimation by varying V_{max} from 5 to 60 mm/s at fixed $M_{max} = 100\ mm$. Each experiment is averaged over 100 trails.

The reconstructed heart sound signal SNR manually computed by the power ratio of the heart sound signals to the non heart sound signal (noise) gives direct measurement of the recovery performance. The higher the V_{max} the poorer the recovery is because the more RBM spectral leakage into the heart sound spectral band Fig.7. An important observation is that heart rate estimation accuracy is not affected much by the cancellation residual, e.g. in Fig. 5(b), due to the increasing speed of RBM. In particular, estimation root-mean-squared-error (RMSE) is constant at 0.6 beats/min (bpm) at different V_{max} Fig.7. The desirable result is feasible because the new heart rate estimation methodology based on heart sound signal recovery, further enhanced by the active motion cancellation technique.

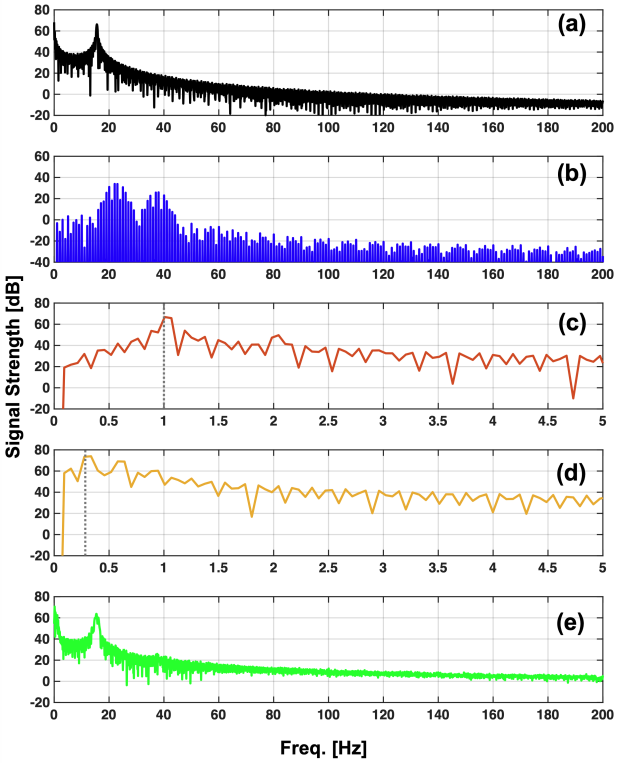

Fig. 4. Spectra of the signals in Fig. 3 at the radar receiver assuming independently present. (a) RBM; (b) heart sound; (c) heartbeat; (d) respiration; and (e) mixed signal of (a)-(d). Vertical lines in (c)(d) denote the heartbeat and respiration frequencies, respectively.

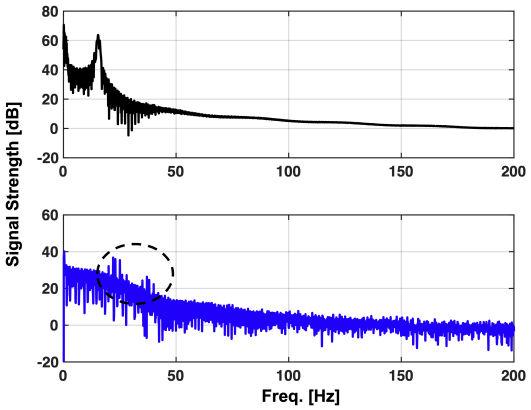

Fig. 5. Spectra of the estimated RBM in Fig. 4(a) and the RBM suppressed revealing heart sound spectral features, highlighted by the circle.

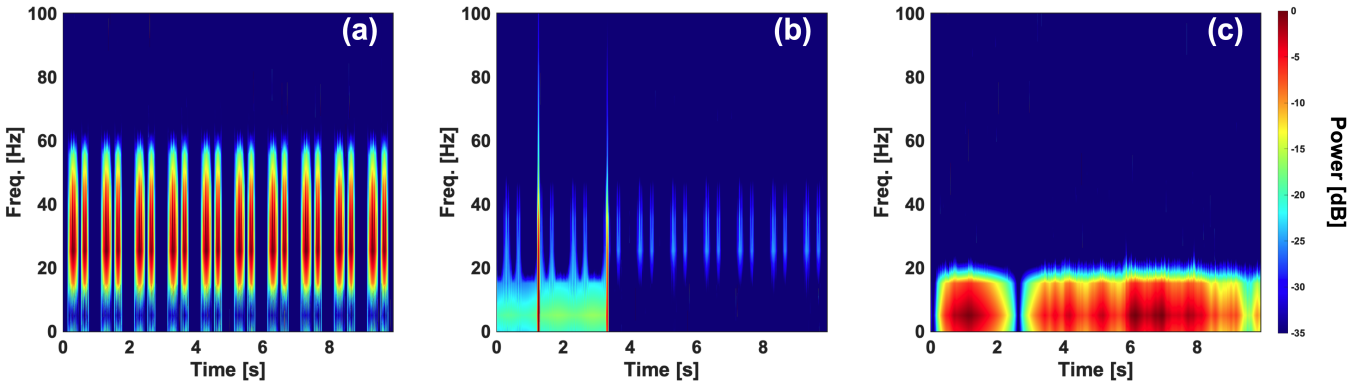

Fig. 6. Heart sound spectrogram. (a) true; (b) motion-cancelled; (c) high-pass filtered. Results (b)(c) are generated when the RBM occurs with $V_{max} = 60\ mm/s$ and $M_{max} = 100\ mm$.

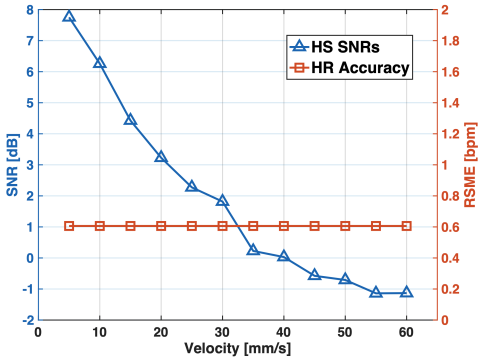

Fig. 7. Heart sound recovery in terms of SNR and robust heart rate estimation accuracy as a function of RBM velocity from 5 to 60 mm/s given the maximum RBM bounded by 100 mm.

VI. Remarks

This paper presented a novel wideband radar signal processing method for robust heart rate estimation in presence of large-scale RBM. Such capability is enabled by 1) a motion cancellation technique operated in complex signal domain insensitive to phase calibration compared to conventional methods and 2) a radar heart sound based heart rate estimation strategy leveraging spectral separation and its resilience to motion interference in time-frequency domain.

The simulated study showed encouraging results of the new methodology. Actual Human subject test and system validation will be performed in the future.

References

[1] I. Lenz, Y. Rong, and D. Bliss, "Contactless stethoscope enabled by radar technology," *Bioengineering*, vol. 10, no. 2, p. 169, 2023.

[2] I. Immoreev and T.-H. Tao, "UWB radar for patient monitoring," *IEEE Aerospace and Electronic Systems Magazine*, vol. 23, no. 11, pp. 11–18, 2008.

[3] C. Li, V. M. Lubecke, O. Boric-Lubecke, and J. Lin, "A review on recent advances in Doppler radar sensors for noncontact healthcare monitoring," *IEEE Transactions on Microwave Theory and Techniques*, vol. 61, no. 5, pp. 2046–2060, 2013.

[4] M. Mercuri, I. R. Lorato, Y.-H. Liu, F. Wieringa, C. V. Hoof, and T. Torfs, "Vital-sign monitoring and spatial tracking of multiple people using a contactless radar-based sensor," *Nature Electronics*, vol. 2, no. 6, pp. 252–262, 2019.

[5] C. Li and J. Lin, "Random body movement cancellation in doppler radar vital sign detection," *IEEE Transactions on Microwave Theory and Techniques*, vol. 56, no. 12, pp. 3143–3152, 2008.

[6] C. Gu, G. Wang, Y. Li, T. Inoue, and C. Li, "A hybrid radar-camera sensing system with phase compensation for random body movement cancellation in doppler vital sign detection," *IEEE transactions on microwave theory and techniques*, vol. 61, no. 12, pp. 4678–4688, 2013.

[7] Y. Rong, A. Dutta, A. Chiriyath, and D. W. Bliss, "Motion-tolerant non-contact heart-rate measurements from radar sensor fusion," *Sensors*, vol. 21, no. 5, p. 1774, 2021.

[8] F.-K. Wang, T.-S. Horng, K.-C. Peng, J.-K. Jau, J.-Y. Li, and C.-C. Chen, "Single-antenna doppler radars using self and mutual injection locking for vital sign detection with random body movement cancellation," *IEEE Transactions on Microwave Theory and Techniques*, vol. 59, no. 12, pp. 3577–3587, 2011.

[9] Q. Lv, D. Ye, S. Qiao, Y. Salamin, J. Huangfu, C. Li, and L. Ran, "High dynamic-range motion imaging based on linearized doppler radar sensor," *IEEE Transactions on Microwave Theory and Techniques*, vol. 62, no. 9, pp. 1837–1846, 2014.

[10] B.-K. Park, O. Boric-Lubecke, and V. M. Lubecke, "Arctangent demodulation with dc offset compensation in quadrature doppler radar receiver systems," *IEEE transactions on Microwave theory and techniques*, vol. 55, no. 5, pp. 1073–1079, 2007.

[11] I. Lenz, Y. Rong, and D. W. Bliss, "Radarcardiograph Signal Modeling and Time-Frequency Analysis," in *2023 IEEE Radar Conference*. IEEE, 2023, in press.

[12] Y. Rong, K. V. Mishra, and D. W. Bliss, "Novel respiration-free heartbeat detection algorithm using millimeter wave radar," in *2022 56th Asilomar Conference on Signals, Systems, and Computers*. IEEE, 2022, in press.

[13] K. Han and S. Hong, "Phase-extraction method with multiple frequencies of fmcw radar for human body motion tracking," *IEEE Microwave and Wireless Components Letters*, vol. 30, no. 9, pp. 927–930, 2020.

[14] J. Wang, X. Wang, L. Chen, J. Huangfu, C. Li, and L. Ran, "Noncontact distance and amplitude-independent vibration measurement based on an extended dacm algorithm," *IEEE Transactions on Instrumentation and Measurement*, vol. 63, no. 1, pp. 145–153, 2013.